Supporting Information

Pro-Inflammatory and Pro-Fibrogenic Effects of Ionic and Particulate Arsenide and Indium-Containing Semiconductor Materials in the Murine Lung

Wen Jiang[†], Xiang Wang[†], Olivia J. Osborne[†], Yingjie Du[†], Chong Hyun Chang[†], Yu-Pei Liao[‡], Bingbing Sun[†], Jinhong Jiang[†], Zhaoxia Ji[†], Ruibin Li[†§], Xiangsheng liu[‡], Jianqin Lu[‡], Sijie Lin[†◊], Huan Meng[‡], Tian Xia[†‡] and André E. Nel[†‡*]

[†] Center for Environmental Implications of Nanotechnology, California NanoSystems Institute, University of California Los Angeles, 570 Westwood Plaza, Los Angeles, CA 90095, United States;

[‡] Division of NanoMedicine, Department of Medicine, University of California Los Angeles, 10833 Le Conte Ave, Los Angeles, CA 90095, United States;

[◊] College of Environmental Science and Engineering State Key Laboratory of Pollution Control and Resource Reuse, Tongji University, Shanghai, China, 200092

[§] School of Radiation Medicine and Protection & School for Radiological and Interdisciplinary Sciences (RAD-X), Medical College of Soochow University, Suzhou, Jiangsu 215123, China

[*]Address correspondence to:

André E. Nel, M.D./Ph.D.

Department of Medicine, Division of NanoMedicine, UCLA School of Medicine, 52-175 CHS, 10833 Le Conte Ave, Los Angeles, CA 90095-1680, USA

Tel: (310) 825-6620, Fax: (310) 206-8107

E-mail: *anel@mednet.ucla.edu*

Materials and Methods

ICP-OES Analysis to Determine III-V Particles Dissolution in the Lung Simulated Fluids: ICP-OES was used to assess the release of III-V elements from particles in simulated bronchoalveolar lavage fluid (sBALF) as well as simulated lung interstitial fluid (Gamble's solution) *in vitro*. The stock suspensions of micron- and nano-sized GaAs and InAs particles, at 10 mg/mL, were diluted in sBALF and Gamble's solution to obtain 50 μg/mL suspensions, which were incubated in a humidified atmosphere containing 5% CO_2 at 37 °C for 0, 24 and 40 h. After centrifugation at 15,000 rpm for 60 minutes, the supernatants were transferred to clean tubes (SC475, Environmental Express) for acid digestion. Briefly, 10 mL HNO_3 (65–70%) was used for sample digestion at 80 °C for 6 h, followed by evaporation of all liquids at 95 °C. The dried samples were diluted by 2% (v/v) nitric acid for 3 h to extract the analytes. These extracts were transferred to 15 mL ICP-OES tubes and additional HNO_3 was added to reach a final volume of 8 mL. A calibration curve was established using a standard As, Ga and In solution (Elements Inc., 100 mg/L in 2% HNO_3). Each sample and standard was analyzed in triplicate in the presence of 2% (v/v) nitric acid. All the elements dissolved content was normalized based on the original concentration at 0 h.

Statistical Analysis: All the experiments were performed in triplicate with results expressed as mean ± standard deviation (SD). Statistical significance was evaluated using two-tailed heteroscedastic Student's t-tests according to the TTEST function in Microsoft Excel. Statistically significant results were considered as $p<0.05$.

Supplementary Table

Table S1. Itemized list of 102 human cytokines, chemokines, and acute phase proteins in Proteome Profiler™ Human XL Cytokine Array Kit.

Adiponectin	Endoglin	IL-4	IP-10/CXCL10	RAGE
Aggrecan	Fas Ligand	IL-5	I-TAC/CXCL11	CCL5/RANTES
Angiogenin	FGF basic	IL-6	Kallikrein 3/PSA	RBP4
Angiopoietin-1	FGF-7	IL-8	Leptin	Relaxin-2
Angiopoietin-2	FGF-19	IL-10	LIF	Resistin
BAFF	Flt-3 Ligand	IL-11	Lipocalin-2/NGAL	SDF-1 alpha
BDNF	G-CSF	IL-12 p70	MCP-1/CCL2	Serpin E1/PAI-1
Complement Component C5/C5a	GDF-15	IL-13	MCP-3/CCL7	SHBG
CD14	GM-CSF	IL-15	M-CSF	ST2
CD30	GRO α	IL-16	MIF	TARC
CD40 Ligand	Growth Hormone (GH)	IL-17A	MIG/CXCL9	TFF3
Chitinase 3-like 1	HGF	IL-18 BPa	MIP-1 alpha/beta	TfR
Complement Factor D	ICAM-1/CD54	IL-19	MIP-3 alpha	TGF-alpha
C-Reactive Protein/CRP	IFN-gamma	IL-22	MIP-3 beta	Thrombospondin-1
Cripto-1	IGFBP-2	IL-23	MMP-9	TNF-alpha
Cystatin C	IGFBP-3	IL-24	Myeloperoxidase	uPAR
Dkk-1	IL-1 alpha	IL-27	Osteopontin (OPN)	VEGF
DPPIV	IL-1 beta	IL-31	PDGF-AA	Vitamin D BP
EGF	IL-1ra	IL-32 alpha/beta/gamma	PDGF-AB/BB	
EMMPRIN	IL-2	IL-33	Pentraxin 3/TSF-14	
ENA-78	IL-3	IL-34	PF4	

Supplementary Figures

Figure S1

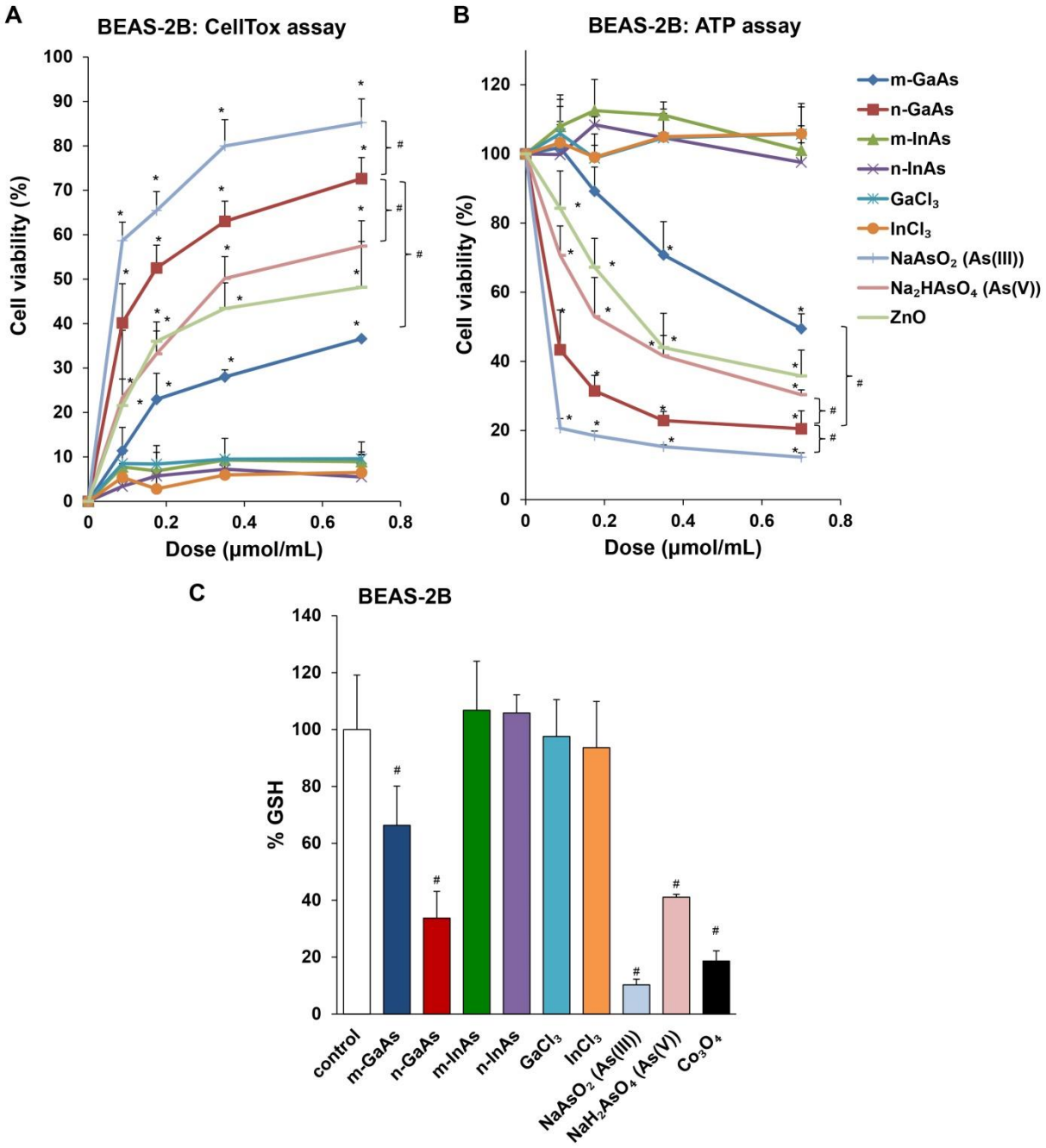

Figure S1. Assessment of cell viability and GSH content in BEAS-2B cells following exposure to III-V particles and ionic forms. (A) Assessment of BEAS-2B cell death by the CellTox assay. (B) Assessment of BEAS-2B cell viability by the ATP assay. The III-V materials were added to

the cell culture media at 0.07-0.7 μmol/mL for 24 h. The corresponding mass doses are listed in Table 3. (*) $p < 0.05$ compared to control; (#) $p < 0.05$ compared to n-GaAs. (C) Intracellular GSH depletion in BEAS-2B cells was determined by luminescence-based GSH-Glo kit. The cells were exposed to III-V materials at 0.35 μmol/mL (=50 μg/mL GaAs) for 24 h. GSH abundance was calculated as the fractional luminescence intensity of treated *versus* untreated cells (in which the abundance was regarded as 1.0). (#) $p < 0.05$ compared to BEAS-2B control cells.

Figure S2

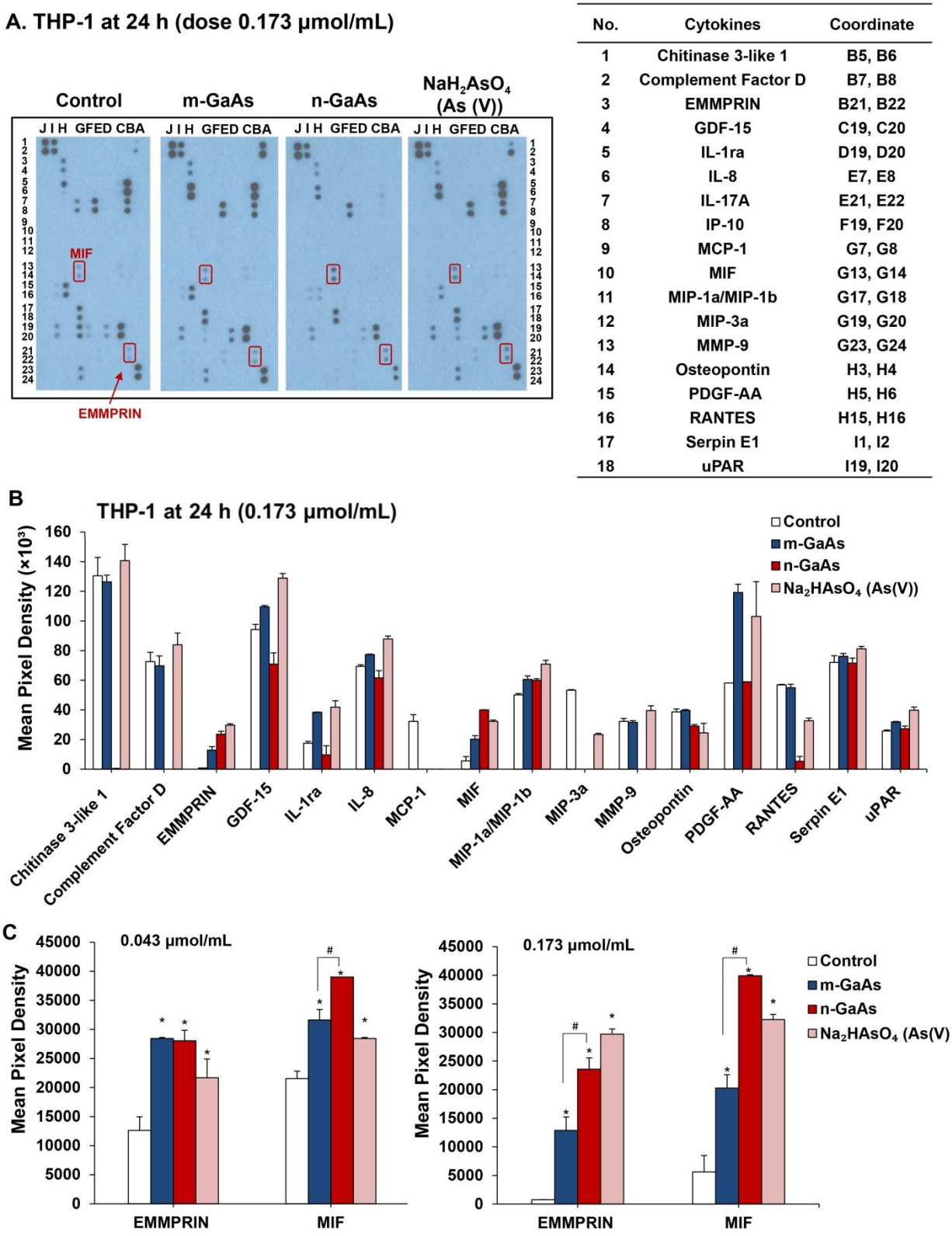

No.	Cytokines	Coordinate
1	Chitinase 3-like 1	B5, B6
2	Complement Factor D	B7, B8
3	EMMPRIN	B21, B22
4	GDF-15	C19, C20
5	IL-1ra	D19, D20
6	IL-8	E7, E8
7	IL-17A	E21, E22
8	IP-10	F19, F20
9	MCP-1	G7, G8
10	MIF	G13, G14
11	MIP-1a/MIP-1b	G17, G18
12	MIP-3a	G19, G20
13	MMP-9	G23, G24
14	Osteopontin	H3, H4
15	PDGF-AA	H5, H6
16	RANTES	H15, H16
17	Serpin E1	I1, I2
18	uPAR	I19, I20

Figure S2. Proteome Profiler Human XL Cytokine Array data for 102 cytokines released from

THP-1 cells 24 h after incubation with 0.173 μmol/mL micron- and nano-sized GaAs, as well as NaH_2AsO_4 (As (V)). (A) X-ray analysis of cytokine array films (left) after 2 minutes of exposure. 100 μL of cell culture supernatant was run for duplicate dots for each array. Pixel density spots were created using an Epson Perfection V500 Photo Scanner and ImageJ 1.46r analysis software. Altogether 18 human cytokines could be detected in THP-1 supernatants (right), among which there were pixel density increases for EMMPRIN (B21, B22) and MIF (G13, G14). (B) Semi-quantitative expression of the pixel density of the 18 cytokines by ImageJ analysis. (C) Semi-quantitative expression of the pixel densities of EMMPRIN and MIF level at exposure doses of 0.043 and 0.173 μmol/mL. (*) $p < 0.05$ compared to control. (#) $p < 0.05$ compared to n-GaAs.

Figure S3

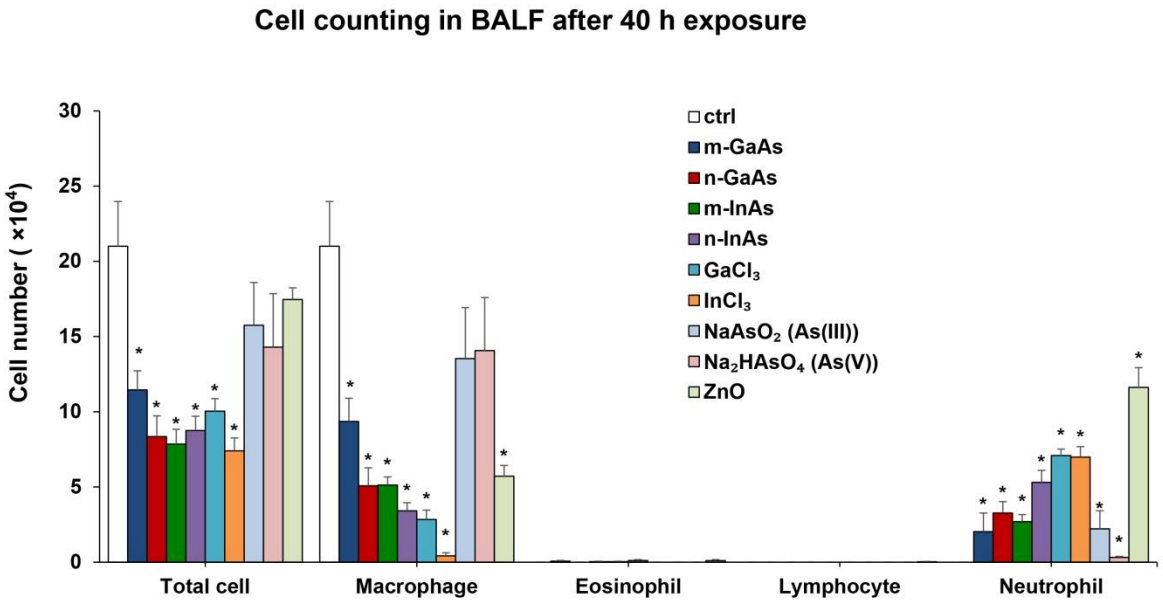

Figure S3. Acute pulmonary effects of III-V materials, 40 h following exposure to a dose of 0.014 mmol/kg. Differential cell counts were performed in the BALF. These data were collected from the same experiment described in Figure 4. There were 6 C57BL/6 mice in each group. Animals were euthanized after 40 h to collect the BALF. ZnO served as a positive control. Exposure to micron- and nano-sized GaAs and InAs particles, $GaCl_3$ and $InCl_3$ led to a significant reduction of the total and macrophage cell counts compared to control or the As(III) and As(V) treated groups. All the III-V materials triggered an increase in neutrophil counts. (*) $p < 0.05$ compared to control.

Figure S4

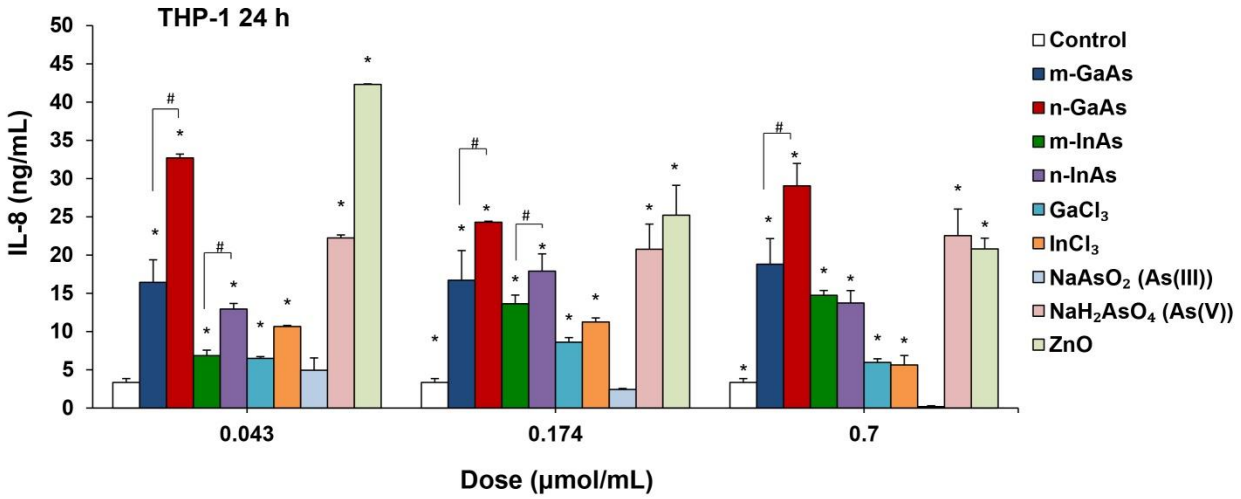

Figure S4. IL-8 production in THP-1 cells. After 24 h, cells were exposed to the particulate and ionic III-V materials at concentrations of 0.043, 0.174 and 0.7 µmol/mL. The corresponding mass doses are listed in Table 3. ZnO NPs were used as a positive control. IL-8 levels in the cell culture supernatant were determined by ELISA. (*) $p < 0.05$ compared to control. (#) $p < 0.05$ compared to nano-sized III-V particles.

Figure S5

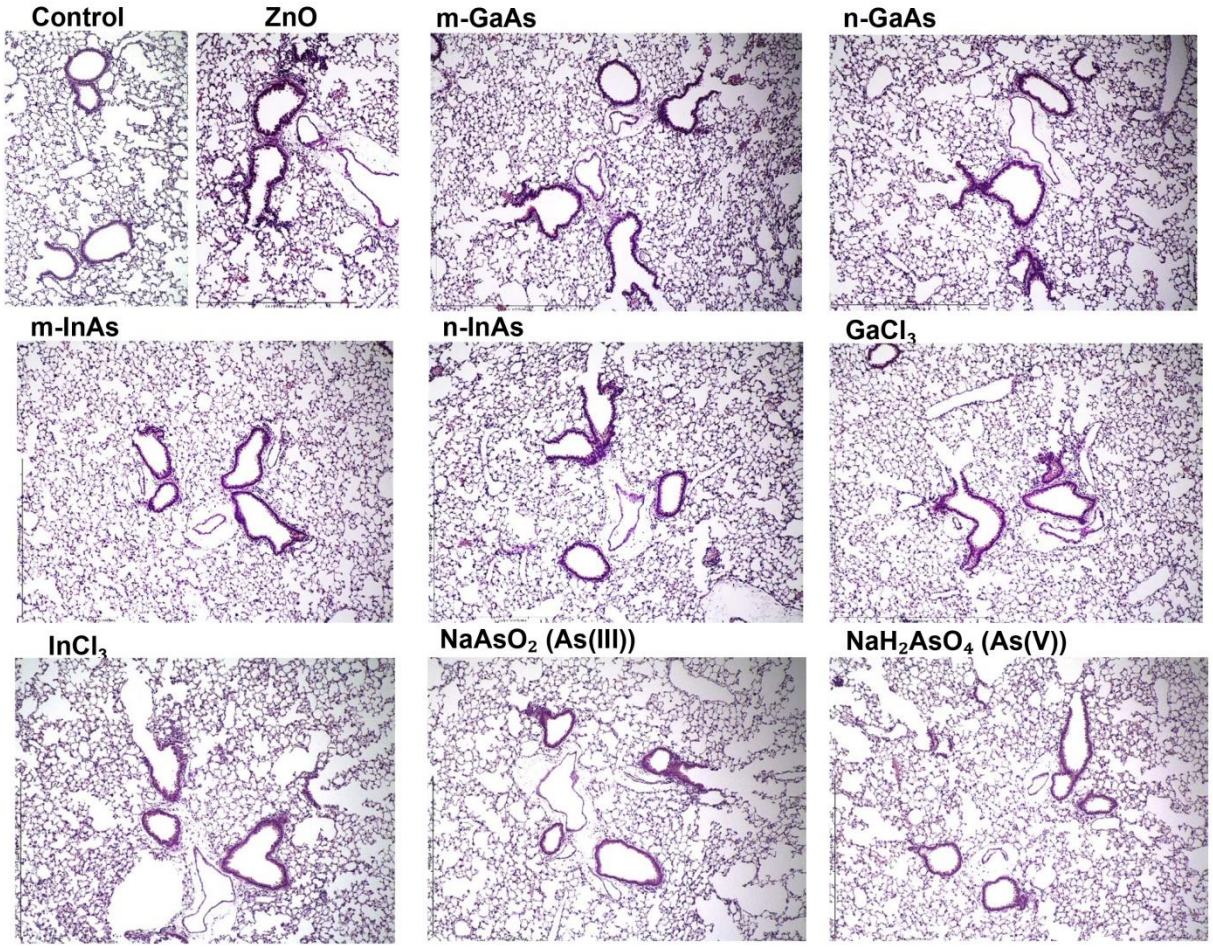

Figure S5. Tissue sectioning and H&E staining of the lungs 40 h after exposure to III-V materials. The selected images at 100× magnification are representative of the histological response in each group.

Figure S6

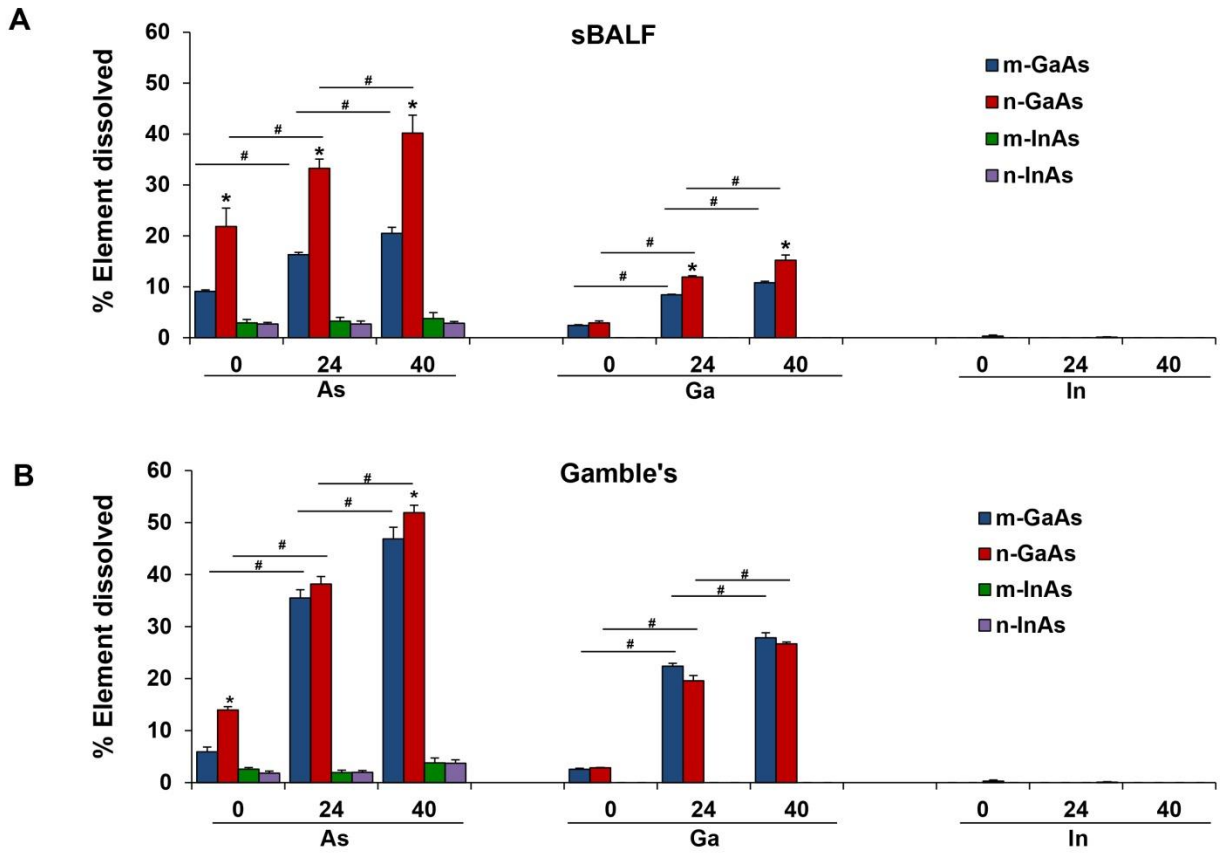

Figure S6. ICP-OES analysis to determine the dissolution of micron- and nano-sized GaAs and InAs at 0, 24 and 40 h in simulated bronchoalveolar lavage fluid (sBALF) (A) as well as simulated interstitial lung fluid (Gamble's solution) (B). (*) $p < 0.05$ compared to control. (#) $p < 0.05$ compared to 24 h incubation.

Figure S7

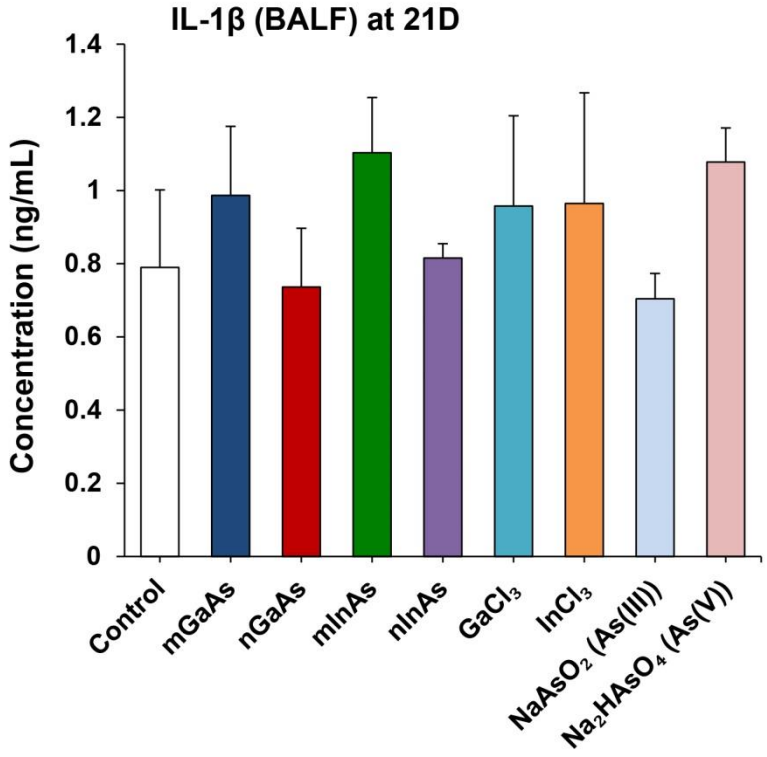

Figure S7. IL-1β levels in the BALF of mice 21 days after oropharyngeal installation of the indicated materials at 0.014 mmol/kg (=2 mg/kg GaAs). The corresponding mass doses are listed in Table 3. These data were collected from the same experiment as in Figure 6. There were 6 animals per group. Animals were euthanized 21 D after initial exposure to collect the BALF. IL-1β levels were determined by ELISA. There was no significant difference for the IL-1β production among III-V materials compared to control group.

Figure S8

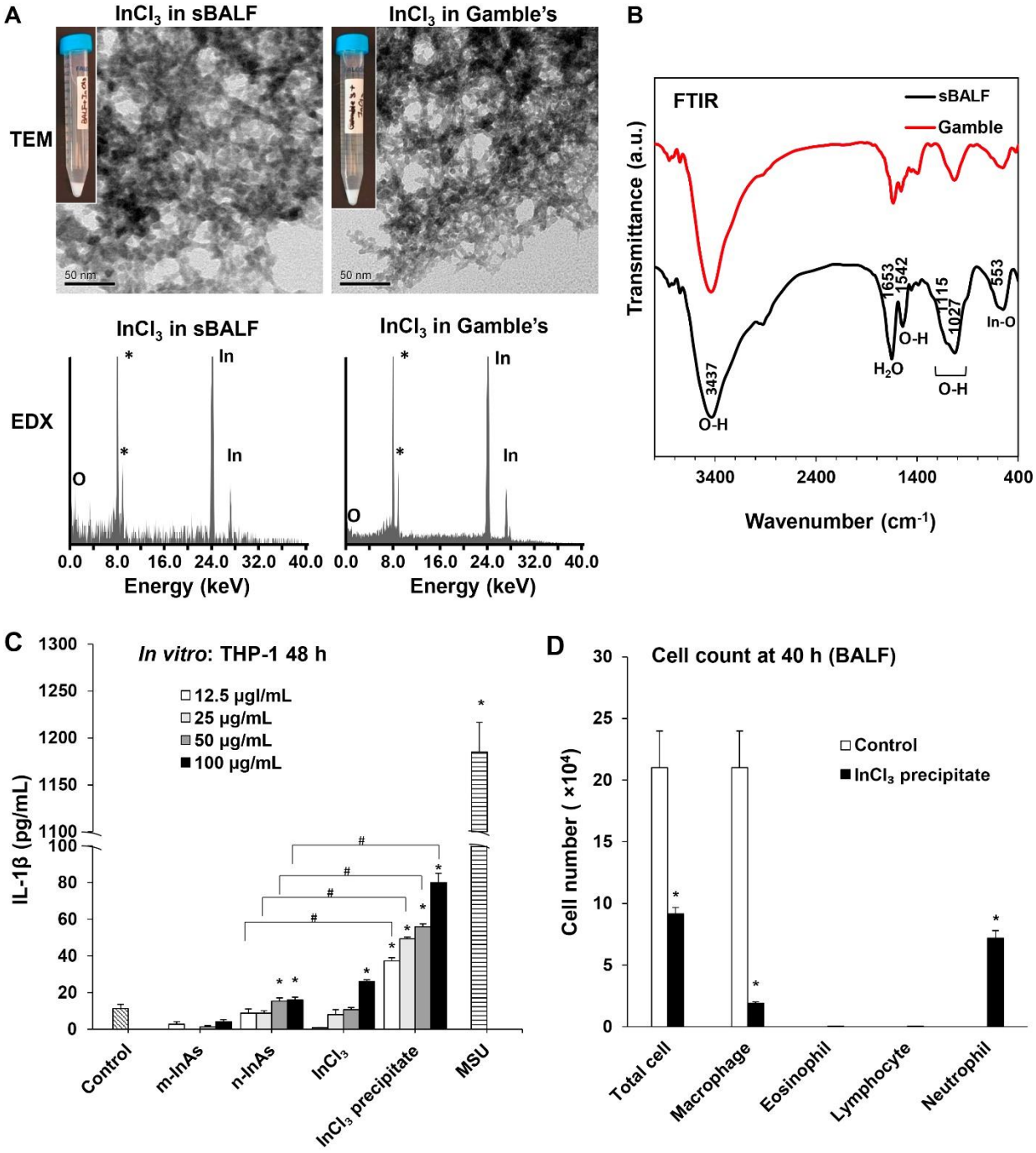
A
InCl3 in sBALF
InCl3 in Gamble's
TEM
50 nm
50 nm
InCl3 in sBALF
InCl3 in Gamble's
EDX
O
In
In
O
In
In
0.0 8.0 16.0 24.0 32.0 40.0
Energy (keV)
0.0 8.0 16.0 24.0 32.0 40.0
Energy (keV)
B
FTIR
sBALF
Gamble
Transmittance (a.u.)
3437
O-H
1653
1542
O-H
H2O
1115
1027
O-H
553
In-O
3400 2400 1400 400
Wavenumber (cm-1)
C
In vitro: THP-1 48 h
12.5 μgl/mL
25 μg/mL
50 μg/mL
100 μg/mL
IL-1β (pg/mL)
1300
1250
1200
1150
1100
100
80
60
40
20
0
Control
m-InAs
n-InAs
InCl3
InCl3 precipitate
MSU
D
Cell count at 40 h (BALF)
Control
InCl3 precipitate
Cell number (×10⁴)
30
25
20
15
10
5
0
Total cell
Macrophage
Eosinophil
Lymphocyte
Neutrophil

Figure S8

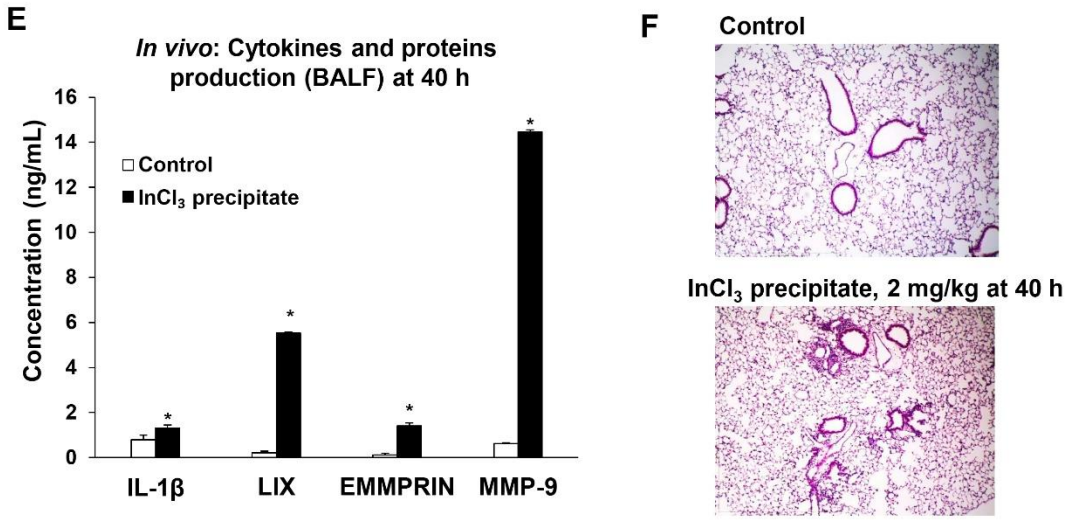

Figure S8. Formation of insoluble $In(OH)_3$ precipitates in simulated bronchoalveolar lavage fluid (sBALF) and simulated interstitial lung fluid (Gamble's solution), as well as their pulmonary effects in the murine lung. (A) TEM and EDX characterization of $InCl_3$ precipitates in sBALF and Gamble's solution *in vitro*. The precipitates were collected by centrifugation 24 h after the incubation in each of the simulated fluids. The precipitates were re-suspended at 50 μg/mL and applied to TEM grids using a JEOL 2010 microscope operated at 200 keV. Scale bars represent 50 nm. EDX demonstrated that the precipitates contained In and O only. (B) FTIR characterization confirmed that the precipitates formed in sBALF and Gamble's solution (*in vitro*) were $In(OH)_3$. (C) $InCl_3$ precipitates in sBALF induced higher IL-1β production than InAs and $InCl_3$ in THP-1 cells after 48 h exposure. (*) $p < 0.05$ compared to control. (#) $p < 0.05$ compared to n-InAs. (D) Acute pulmonary effects of $InCl_3$ precipitates as reflected by differential cell counts in the BALF after 40 h. Anesthetized C57BL/6 mice were exposed to $InCl_3$ precipitates at 2 mg/kg by oropharyngeal aspiration. There were 6 animals per group. Animals were euthanized after 40 h, and BALF was collected to determine differential cell counts. (*) $p < 0.05$ compared to control. (E) IL-1β, LIX, EMMPRIN and MMP-9 levels in BALF as determined by ELISA assay. (*) $p < 0.05$ compared to control. (F) H&E stained images (at 100 ×) of mice lungs exposed to $InCl_3$ precipitates at the dose of 2 mg/kg.

Supplementary Results and Discussion

The pro-fibrogenic effects of $InCl_3$ likely contribute to the pulmonary effects of InAs particles. Even though both Ga and In belong to group III in the periodic table, their biological effects differ.[1-3] Based on the presence of In in the lung tissue by ICP-OES analysis after 48 h and 21 D (Figure 4F, Figure 7C), we hypothesized that the formation of insoluble In compounds could lead to the deposition of a biopersistent In species in the lung. In order to address this theory, Visual MINTEQ software was used to model the chemical speciation of $InCl_3$ in the simulated lung fluids (sBALF and Gamble's solution). This analysis suggests the formation of insoluble $In(OH)_3$ in both media, which constitutes >99.9% of the In content. In contrast, Ga leads to the formation of ionic form $Ga(OH)_4^-$ (>99.9%) in both media. The phase transition of $InCl_3$ to insoluble $In(OH)_3$ could play an important role in $InCl_3$ toxicity *in vivo*. Using TEM, Energy-dispersive X-ray spectroscopy (EDX) and FTIR characterization (Figure S8A-S8B), we demonstrated that $InCl_3$ indeed leads to the formation of nanoscale $In(OH)_3$ precipitates in sBALF and Gamble's solution. The pro-inflammatory potential of $InCl_3$ precipitates was demonstrated by the ability of this material to induce IL-1β production in THP-1 cells (Figure S8C). Moreover, oropharyngeal aspiration in mice demonstrates after 40 h the presence of $InCl_3$ precipitates increased neutrophil cell counts in the BALF (Figure S8D), along with increased production of IL-1β, LIX, EMMPRIN and MMP-9 (Figure S8E). H&E staining confirmed the pro-IL-1β presence of cellular infiltrates around alveoli and blood vessels in response to $InCl_3$ precipitates (Figure S8F). All considered, we propose that the biopersistence of $In(OH)_3$, following its phase transition from $InCl_3$, leads to pro-fibrotic effects as a result of the production of IL-1β and downstream triggering of pro-fibrogenic growth factors.

Supplementary References

1. Tanaka, A., Toxicity of Indium Arsenide, Gallium Arsenide, and Aluminium Gallium Arsenide. *Toxicol. Appl. Pharmacol.* **2004,** *198*, 405-411.
2. Omura, M.; Tanaka, A.; Hirata, M.; Zhao, M. G.; Makita, Y.; Inoue, N.; Gotoh, K.; Ishinishi, N., Testicular Toxicity of Gallium Arsenide, Indium Arsenide, and Arsenic Oxide in Rats by Repetitive Intratracheal Instillation. *Fundam. Appl. Toxicol.* **1996,** *32*, 72-78.
3. Tanaka, A.; Hisanaga, A.; Hirata, M.; Omura, M.; Makita, Y.; Inoue, N.; Ishinishi, N., Chronic Toxicity of Indium Arsenide and Indium Phosphide to the Lungs of Hamsters. *Fukuoka Acta Medica* **1996,** *87*, 108-115.